ACS APPLIED MATERIALS & INTERFACES

Research Article

www.acsami.org

Controllable Synthesis of Functional Hollow Carbon Nanostructures with Dopamine As Precursor for Supercapacitors

Chao Liu, Jing Wang, Jiansheng Li,* Rui Luo, Jinyou Shen, Xiuyun Sun, Weiqing Han, and Lianjun Wang*

Jiangsu Key Laboratory of Chemical Pollution Control and Resources Reuse, School of Environmental and Biological Engineering, Nanjing University of Science and Technology, Nanjing 210094, People's Republic of China

Supporting Information

ABSTRACT: N-doped hollow carbon spheres (N-HCSs) are promising candidates as electrode material for supercapacitor application. In this work, we report a facile one-step synthesis of discrete and highly dispersible N-HCSs with dopamine (DA) as a carbon precursor and TEOS as a structure-assistant agent in a mixture containing water, ethanol, and ammonia. The architectures of resultant N-HCSs, including yolk−shell hollow carbon spheres (YS-HCSs), single-shell hollow carbon spheres (SS-HCSs), and double-shells hollow carbon spheres (DS-HCSs), can be efficiently controlled through the adjustment of the amount of ammonia. To explain the relation and formation mechanism of these hollow carbon structures, the samples during the different synthetic steps, including polymer/silica spheres, carbon/silica spheres and silica spheres by combustion in air, were characterized by TEM. Electrochemical measurements performed on YS-HCSs, SS-HCSs, and DS-HCSs showed high capacitance with 215, 280, and 381 F g^{-1}, respectively. Moreover, all the nitrogen-doped hollow carbon nanospheres showed a good cycling stability 97.0% capacitive retention after 3000 cycles. Notably, the highest capacitance of DS-HCSs up to 381 F g^{-1} is higher than the capacitance reported so far for many carbon-based materials, which may be attributed to the high surface area, hollow structure, nitrogen functionalization, and double-shell architecture. These kinds of N-doped hollow-structured carbon spheres may show promising prospects as advanced energy storage materials and catalyst supports.

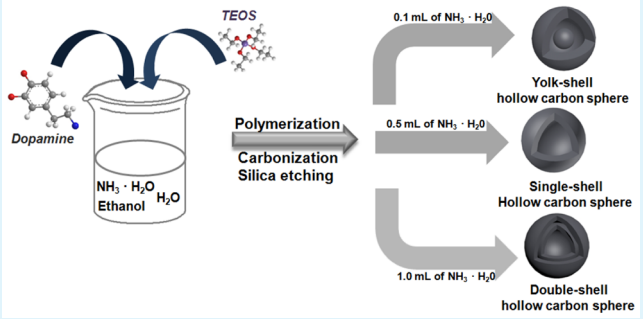

KEYWORDS: *N-doped, hollow carbon spheres, yolk−shell, single-shell, double-shells, structure evolution, supercapacitor*

1. INTRODUCTION

With the rapid development of materials science, substantial research has concentrated on the controllable synthesis of nanomaterials. Among the various architectures of novel materials, hollow carbon spheres (HCSs), including single-shell hollow carbon spheres (SS-HCSs),[1−4] yolk−shell hollow carbon spheres (YS-HCSs),[5−8] and multishell hollow carbon spheres (MS-HCSs),[9−11] have received considerable attention because of their unique structure and functional behavior, such as very high specific area, low specific density, large controllable inner pore volume, and good mechanical strength. Its remarkable properties give it great potential to be applied in the fields of energy storage, water treatment, and biomedicine.[12−22]

For energy storage, HCSs have been widely investigated as the electrode material for the industrialization of supercapacitors due to their advantages, such as high surface areas, shortmass diffusion and transport resistance.[23−25] Recent studies show that functionalizing HCSs with nitrogen groups can significantly increase the surface polarity, electrical conductivity, surface basic sites and electron-donor tendency of the carbon matrix.[26−29] Therefore, great efforts have been devoted to the preparation of N-doped hollow carbon spheres (N-HCSs). In most cases, N-HCSs have been prepared by introducing nitrogen onto carbon frameworks through the post-treatment, for example, treating it with ammonia gas/air, which results in a lower content of nitrogen.[30] To overcome the drawback, N-containing materials (e.g., melamine,[31] phenylenediamine,[32] polyaniline,[33] and acetonitrile[34]) have been employed as carbon precursors for the synthesis of HNCSs. By this route, nitrogen can be preserved at a relatively large content by adjusting the carbonization temperature. However, to date, by that means, it often relies on hard templating strategies, which are commonly carried out with multiple procedures and time-consuming synthetic steps. It is therefore highly desirable to find appropriate carbon precursors and simple approach for the preparation of N-HCSs. Furthermore, it is still a great challenge to synthesize N-HCSs with different architectures including SS-HCSs, YS-HCSs, and MS-HCSs, in a controlled sequence.

Dopamine, a nontoxic, widespread, and sustainable resource, has been proposed as an alternative material in the synthesis and applications of carbon spheres due to its excellent biocompatibility and high carbonization yield. Moreover, the N-doped

Received: June 8, 2015
Accepted: August 5, 2015
Published: August 5, 2015

DOI: 10.1021/acsami.5b05035
ACS Appl. Mater. Interfaces 2015, 7, 18609−18617

nature of dopamine makes it an ideal precursor for nitrogen functional carbon materials.[35−39] On this basis, HNCSs have been synthesized by immersing the silica template in a dopamine tris-buffer solution followed by carbonization and HF etching of the template.[40] This is the first time dopamine has been utilized in the construction of carbon-based nanomaterials. However, the process relies on a hard templating approach, which is complex and fussy. The structure of obtained HNCSs was monotonous and untunable. Recently, Lu and colleagues described a facile synthesis pathway for the generation of monodisperse and size-controlled carbon spheres.[41] In this strategy, polydopamine spheres as a carbon precursor were first prepared through polymerization of dopamine in a mixture containing water, ethanol, and ammonia at room temperature. Then, carbon spheres were obtained by the sequential carbonization process. More recently, Dai et al. reported a successful synthesis of mesoporous carbon spheres (MCNs) using a non-Pluronic amphiphilic block copolymer (PEO-*b*-PS) as a soft template and DA as a precursor.[37] N-Doped MCNs with a large mesopore of 16 nm and small particle size of 200 nm were obtained. Although the above two strategies were facile and efficient, N-doped carbon spheres with hollow structures were hardly to be prepared. Moreover, it is still difficult to synthesize carbon materials with different structures using DA in a controllable system. Therefore, exploring new facile synthetic route for the preparation of hollow carbon materials with tunable structures using dopamine as carbon source is of great significance.

Herein, we report a facile one-step synthesis of discrete and highly dispersible N-doped hollow carbon spheres (N-HCSs) with dopamine (DA) as a carbon precursor and TEOS as a structure-assistant agent, in a mixture containing water, ethanol and ammonia. Carbonization was followed by etching of the silica in the carbon/silica nanocomposite, resulting in the formation of HCSs (Scheme 1). The architectures of resultant

Scheme 1. Formation of N-Doped Hollow Carbon Spheres with Yolk−Shell, Single-Shell, Double-Shells

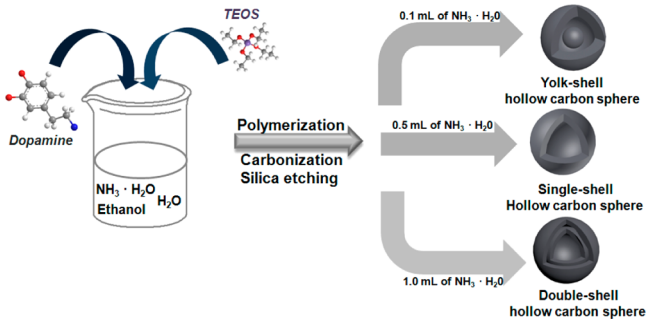

HCSs, including yolk−shell hollow carbon spheres (YS-HCSs), single-shell hollow carbon spheres (SS-HCSs), and double-shells hollow carbon spheres (DS-HCSs), can be efficiently controlled through the adjustment of the amount of ammonia, which can significantly influence the hydrolysis and polymerization rate of TEOS and DA. To demonstrate the benefits of such hierarchical structures in energy storage, we then evaluated supercapacitor performance by using these hollow structured carbons as electrodes. Ascribed to the unique feature of hollow structure, large surface area and high N content, all the three HCSs show remarkable capacitance and outstanding stability.

2. EXPERIMENTAL SECTION

2.1. Chemicals and Materials. Dopamine hydrochloride (DA) was purchased from Sigma-Aldrich. Anhydrous ethanol and tetraethoxysilane (TEOS) were purchased from Sinopharm Chemical Reagent Co., Ltd. Ammonia aqueous solution (25−28%) and hydrofluoric acid solution (40%) was purchased from Nanjing Chemical Reagent Co., Ltd. All chemicals were used as received without any further purification. Millipore water was used in all experiments.

2.2. Synthesis of Single-Shell Hollow Carbon Spheres (SS-HCSs). Typically, ammonia aqueous solution (0.5 mL, 25%) was mixed with a solution containing anhydrous ethanol (12 mL) and water (40 mL), and the mixture was stirred for 30 min. Then, 0.5 mL TEOS was added into the solution and stirred for 15 min. Therefore, the silica core can be preformed. After that, dopamine hydrochloride (0.2 g) was dissolved in water (4 mL). Subsequently, the obtained dopamine hydrochloride solution was added to the above solution and stirred for 36 h at 25 °C. The black products was recovered by centrifugation and air-dried at 60 °C overnight. Calcination was carried out in a tubular at 800 °C in nitrogen at a rate of 5 °C min^{-1}. After removing the silica component by etching in HF solution (10 wt %), SS-HCSs were obtained.

2.3. Synthesis of Yolk−Shell (YS) HCSs and Double-Shell (DS) Hollow Carbon Spheres (HCSs). Typically, ammonia aqueous solution (NH_4OH, 0.1 mL for YS-HCSs, and 1 mL for DS-HCSs) was mixed with a solution containing anhydrous ethanol (12 mL) and water (40 mL), and the mixture was stirred for 30 min. Dopamine hydrochloride (0.2 g) was dissolved in water (4 mL). Subsequently, the obtained dopamine hydrochloride solution and TEOS (0.5 mL) was added to the reaction solution and stirred for 36 h at 25 °C. The black products was recovered by centrifugation and air-dried at 60 °C overnight. Calcination was carried out in a tubular at 800 °C in nitrogen at a rate of 5 °C min^{-1}. After removing the silica component by etching in HF solution (10 wt %), two kinds of carbon materials were obtained, which were donated as YS-HCSs and DS-HCSs, respectively.

2.4. Synthesis of N-Doped Carbon Spheres (NCSs). For comparison, N-doped carbon spheres (NCSs) were also synthesized without adding TEOS, while the other conditions were kept unchanged. The amount of ammonia solution was also tuned, including 0.1, 0.5, and 1 mL. The corresponding carbon spheres were donated as NCSs-1, NCSs-2, and NCSs-3.

2.5. Characterization. TEM (transmission electron microscopy) analysis was conducted on a TECNAI G2 20 LaB6 electron microscope operated at 200 kV. SEM (scanning electron microscopy) analysis was conducted on FEI S4800 system. N_2 adsorption and desorption isotherms were measured using Micromeritics ASAP-2020 at liquid nitrogen temperature (−196 °C). The XPS spectra were obtained by using a PHI Quantera II ESCA System with Al Kα radiation at 1486.8 V. N_2 adsorption/desorption isotherms were measured using Micromeritics ASAP-2020 at liquid nitrogen temperature (−196 °C). TGA measurements were carried out on a SDTQ600 analyzer from 25 to 800 °C under N_2 with a heating rate of 10 °C/min.

2.6. Electrochemical Measurements. All the electrochemical measurements were conducted on a computer-controlled potentiostat (CHI 760C, CH Instrument) with a three-electrode electrochemical cell at 25 °C using a 1 M H_2SO_4 electrolyte. The standard three-electrode electrochemical cell was fabricated using glassy carbon with deposited sample as the working electrode, platinum wire as the counter electrode, and Ag/AgCl as the reference electrode. The working electrodes were fabricated as follows: First, 5 mg of hollow carbon spheres was mixed with 1 mL of DI water/isopropanol (1:1). The obtained suspension (10 μL) was dropped onto a glassy carbon electrode (CHI 104) with diameter of 3 mm. Through measurement, the loading mass of hollow carbon spheres was 50 μg. Normalized by the surface area of the working electrode, the loading mass was 0.7 mg/cm^2. After drying, a Nafion solution (0.5 wt % in isopropyl alcohol) was coated on the sample as the binder. The potentials for electrochemical measurements are reported relative to a Ag/AgCl (saturated KCl) reference electrode and the potential window for cycling was confined between 0 and 0.8 V.

DOI: 10.1021/acsami.5b05035
ACS Appl. Mater. Interfaces 2015, 7, 18609−18617

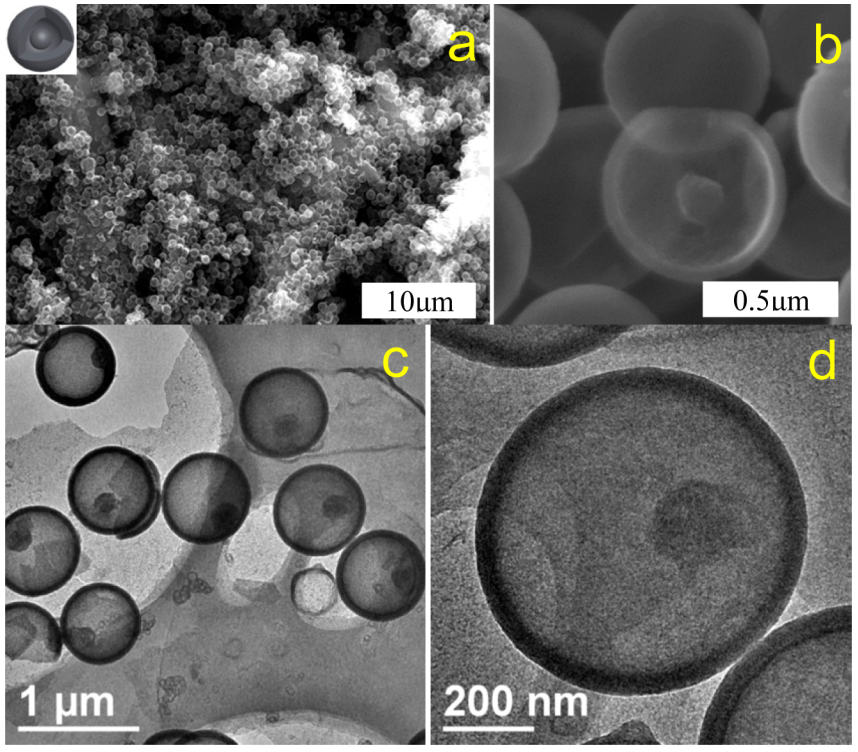

Figure 1. (a and b) SEM images and (c and d) TEM images of YS-HCSs.

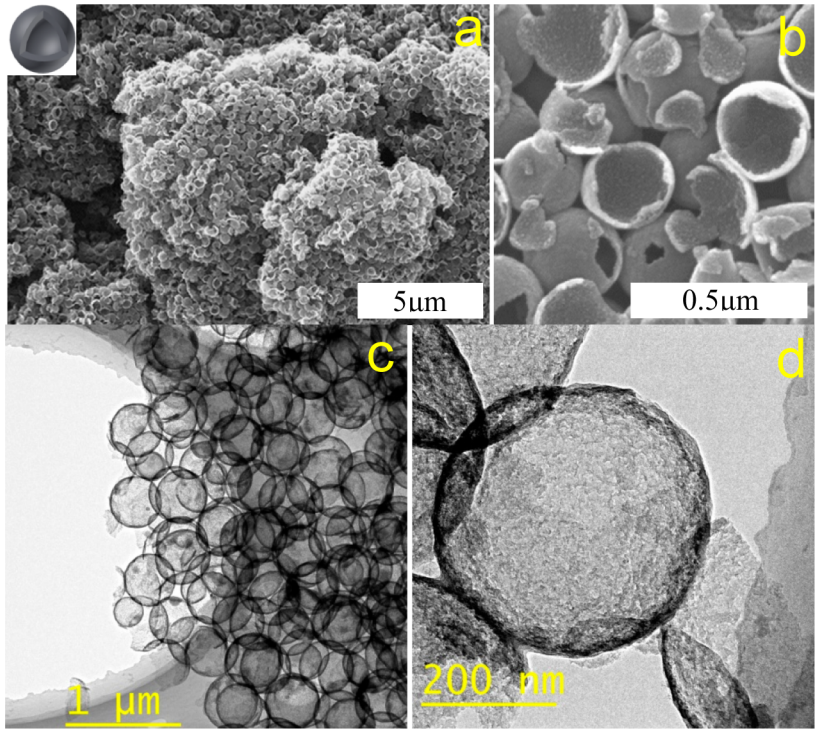

Figure 2. (a and b) SEM images and (c and d) TEM images of SS-HCSs.

3. RESULTS AND DISCUSSION

Yolk−shell structures are powerful platforms for controlled release, confined nanocatalysis, and energy applications.[42] Conventional methods require the fabrication of core/shell nanoparticles, and the synthetic procedures are always multistep and complex. Using our method, yolk−shell carbon spheres with high dispersibility can be easily synthesized. Figure 1a,b show the SEM images of YS-HCSs at varied magnifications, which were formed with adding the smallest amount of ammonia aqueous solution (0.1 mL, 25%). It is found that well-defined and monodispersed nanopsheres of about 760 nm in diameter are present in the large-scale SEM image. At a higher magnification, the carbon yolk with a particle size of ∼175 nm, located in the hollow space, can be clearly observed. The wall thickness

DOI: 10.1021/acsami.5b05035
ACS Appl. Mater. Interfaces 2015, 7, 18609−18617

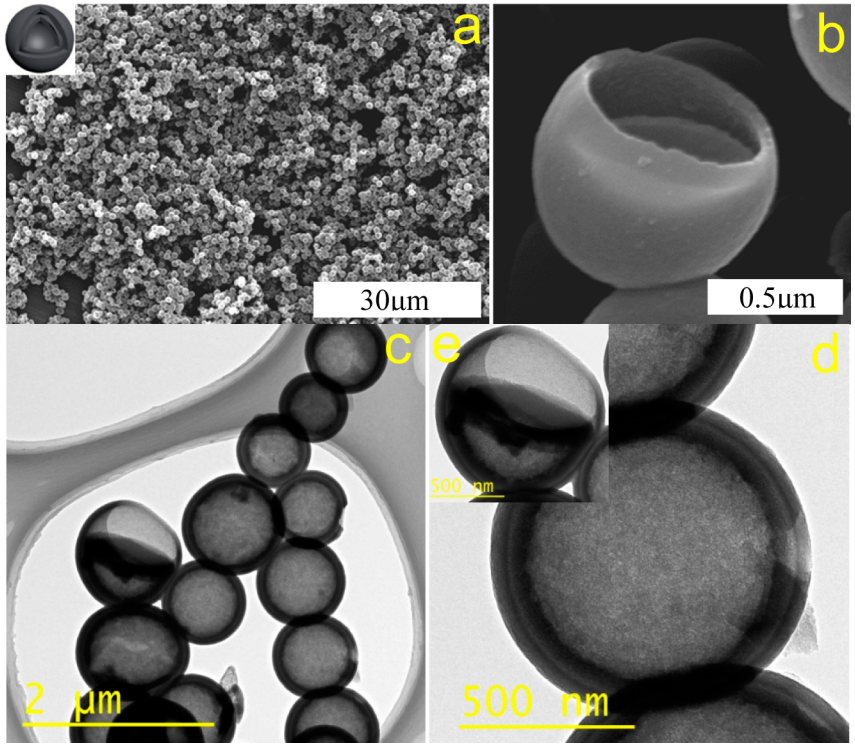

Figure 3. (a and b) SEM images and TEM images (c–e) of DS-HCSs.

measured from the SEM image is ~50 nm. The TEM images of YS-HCSs (Figure 1c,d) show a very uniform yolk–shell particle with a size of ~750 nm, a shell thickness of ~45 nm, and a yolk size of ~180 nm, in accordance with the SEM results. The yolk–shell structure of resultant carbon spheres indicated that the nucleation rate of dopamine was faster than TEOS in this reaction condition. The carbonic cores and shells of these YS-HCSs were confirmed from the TGA curves, from which 100% weight loss was achieved (Figure S1a). These results indicated the successful fabrication of the yolk–shell carbon spheres.

To synthesize hollow carbon spheres with a single shell, we used ammonia aqueous solution (0.5 mL, 25%) to promote the rapid nucleation of silica. To ensure that the silica core could be preformed, we pre-added TEOS into the reaction solution. Then, polydopamine (PDA) as polymer shell could coat the silica cores.[35] After carbonization and silica removal, single-shell hollow carbon spheres were obtained. Homogeneous SS-HCSs with a smooth surface and a diameter of approximately 400 nm are presented in Figure 2a. The hollow-structured morphology was directly proved by the high-magnification SEM image (Figure 2b). The single carbon shell with thickness of about 20 nm was also clearly demonstrated. In addition, some hemispheres and fragments can be observed. The ultrathin outer shell may be unstable and broken during the carbonizing and silica etching process, leading to the structure damage. As shown in Figure 2c and d, the remarkable feature of the spheres is the obvious contrast between the dark edge and the pale center, as is reported for other hollow particles with a central cavity.[5] It is observed that the resultant SS-HCSs have very thin shell with thickness of ~22 nm and large cavity with size of ~340 nm, which is consistent with the SEM measurements. The TGA result of SS-HCSs confirmed the carbon framework (Figure S1b). Therefore, it can be concluded that N-doped hollow carbon spheres with single shell have been facilely prepared.

When more ammonia aqueous solution (1.0 mL) was added into the reaction solution, the structure of carbon spheres were transformed from hollow structure with single shell to double shells. From the SEM images, the as-synthesized DS-HCSs are seen to exhibit a monodispersed spherical morphology with a diameter of 750–910 nm (Figure 3a). The hollow cavity and two-layer lamellar structure can be clearly identified from a broken hemisphere (Figure 3b). Compared with SS-HCSs, the spherical morphology of DS-HCSs was well preserved after carbonization and silica removal, which may be contributed to the thicker shell thickness and double-shells structure. The TEM image further confirmed the hollow and double-shell structure of DS-HCSs (Figure 3c–e). The shell thickness and interlayer distance were about 46 and 15 nm, respectively, which were measured through the HRTEM. The weight loss of DS-HCSs can achieved 100% in air, indicating the total removal of silica and a carbonic framework. Therefore, in our synthesis system, DS-HCSs with N-functionalization can be facilely fabricated.

The N_2 sorption isotherms of the obtained three hollow carbon spheres are shown in Figure S2. The BET surface areas of YS-HCSs, SS-HCSs and DS-HCSs are 427, 622, and 822 m^2/g, respectively, and the total pore volumes are 0.28, 0.48, and 0.47 $cm^3\ g^{-1}$, respectively. The sharp increase in N_2 uptake at P/P_0 = 0.9–1.0 corresponds to the hollow cavity, in agreement with the SEM and TEM results. X-ray photoelectron spectroscopy (XPS) is a powerful technique for the characterization of elemental composition and bonding configuration in materials. Figure S3 is the XPS survey spectra of YS-HCSs, SS-HCSs, and DS-HCSs, which shows the peaks of C 1s, O 1s, and N 1s. The content of nitrogen in these materials is listed in Table S1. The as-synthesized three kinds of carbon spheres have the similar nitrogen form in the carbon matrix due to the same carbon precursor and carbonization temperature. The high-resolution XPS spectra of N 1s can be curve-fitted into four-type peaks (Figure 4a), which are correlated to different electronic states of

DOI: 10.1021/acsami.5b05035
ACS Appl. Mater. Interfaces 2015, 7, 18609–18617

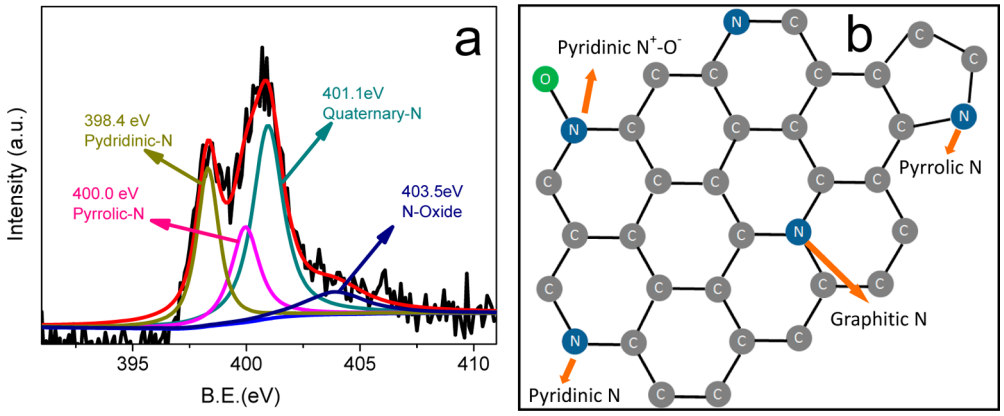

Figure 4. (a) High-resolution N 1s spectrum of the as-synthesized N-HCSs and (b) relative contents of nitrogen species.

the nitrogen functional groups: pyridinic N (398.6 eV), pyrrolic N (400 eV), graphitic N (400.9 eV), and pyridine N-oxide (N-X, 403 eV) (Figure 4b), implying the successful doping of N in these materials. The Raman spectrum shows two peaks at around 1350 and 1580 cm^{-1}, which are in accordance with the disordered carbon (D-bond) and the graphitic carbon (G-bond), respectively (Figure S4). The presence of G-band indicated the graphitic nature of the N-doped carbon spheres, which is favorable for the electrical conductivity enhancement. This observation is corresponding to the reported works[41,43] using dopamine as carbon precursor.

To demonstrate the structure-assistant role of silica, we prepared N-doped carbon spheres (NCSs) without adding TEOS. Unlike N-HCSs, the NCSs possess a solid spherical morphology, not a hollow structure (Figure S5), similar to the previous report.[41] The particle size of NCSs-1, NCSs-2, and NCSs-3 was measured to be 1000, 300, and 180 nm. Therefore, the particle size of NCSs was decreased with increasing the amount of ammonia, without structure changes. The results further prove that TEOS played the role of structure-assistant agent in the formation of N-HCSs.

To acquire more information on the structure evolution of the three N-HCSs, we employed TEM during the different synthetic step to characterize the sampless, including polymer/silica spheres (PSSs), carbon/silica spheres (CSSs), and silica spheres (SSs) by combustion CSSs in air. TEM images of PSSs, CSSs, and SSs, corresponding to YS-HCSs, were shown in Figure S6. The yolk−shell morphology of YS-PSSs, with a core−void−shell−shell structure, can be clearly seen (Figure S6a). After carbonization, YS-CSSs kept the core−void−shell−shell structure (Figure S6b). The hollow structure of YS-SSs by removing carbon further indicated the carbonic core and outer shell of YS-HCSs (Figure S6c). The particle size of YS-SSs (660 nm) and core size of YS-CSSs (170 nm) was consistent with the cavity size and core diameter of YS-HCSs, respectively. Figure S7a,b shows the TEM image of SS-PSSs and SS-CSSs, corresponding to SS-HCSs, from which hollow morphology with void−shell−shell structure was observed. Similar to YS-SSs, hollow SSs can be obtained by removal the carbon of SS-CSSs (Figure S7c). The diameter of SS-SSs was measured to be 340 nm, in accordance with the cavity size of SS-HCSs. For DS-HCSs, TEM images of DS-PSSs and DS-CSSs also possessed the void−shell−shell structure, with a hollow structure of DS-SSs after carbon removal (Figure S8). It can be seen that an outer shell (45 nm), a pale layer (18 nm), and a darker inner layer (56 nm) corresponding to the outer shell, interlayer, and inner shell of DS-HCSs, appeared in the sample of DS-CSSs after carbonization.

On the basis of above observations, we proposed the formation process and relation of the three N-HCSs as follows: In the condition of synthesizing YS-HCSs by using smallest amount of ammonia aqueous solution, the polymerization of DA is much faster than that of TEOS at the initial stage, leading to the core formation, similar to the resorcinol-formaldehyde/silica assembly system for yolk−shell carbon spheres.[44] With the sol−gel process prolonged, the concentration of DA is gradually decreased, resulting in the gradient hydrolysis and condensation of silicates. The generated silicate oligomers form the interlayer. With continuous consuming, the hydrolysis rate of TEOS will be drastically reduced. Until the polymerization of DA becomes faster again, the residual PDA will be further deposited on the silica surface, resulting in the generation of core−void−shell−shell YS-PSSs. Thus, the yolk−shell structured N-HCSs can be fabricated after carbonization and silica etching. To synthesize SS-HCSs, we preadded a relatively large amount of ammonia aqueous solution and TEOS to the synthesis system. The hydrolysis and condensation of TEOS first occurs, leading to the formation of silica core. After adding DA, the polymerization is initiated. Then, PDA as polymer shell is coated on the silica cores, forming the void−shell−shell SS-PSSs. Through heat treatment and silica etching process, N-HCSs with single shell can be obtained. In the process of synthesizing DS-HCSs, more ammonia aqueous solution is used with the simultaneous addition of TEOS and DA. In this case, the hydrolysis and condensation of TEOS is faster than the polymerization of DA. Therefore, the silica core was preferentially generated. The concentration of TEOS is decreased with the reaction proceeding, resulting in a slower polymerization rate that well matched the polymerization rate of DA. The silicate oligomers from the hydrolysis of TEOS together with PDA polymer can codeposite at the surface of the silica core, thereby creating the silica/PDA composite shell. With the further decrease of the TEOS concentration, the polymerization of DA becomes the main reaction, resulting in the formation of a PDA shell on the silica/PDA composite shell. The void−silica−silica/PDA−PDA structured DS-PSSs are finally formed. During the pyrolysis process, the void−silica−silica/PDA−PDA structure is transformed to void−silica−silica/carbon−silica−carbon structure due to the thermal shrinkage of polymer.[37] Thus, through carbonization and silica etching, double-shells N-HCSs are obtained.

DOI: 10.1021/acsami.5b05035
ACS Appl. Mater. Interfaces 2015, 7, 18609−18617

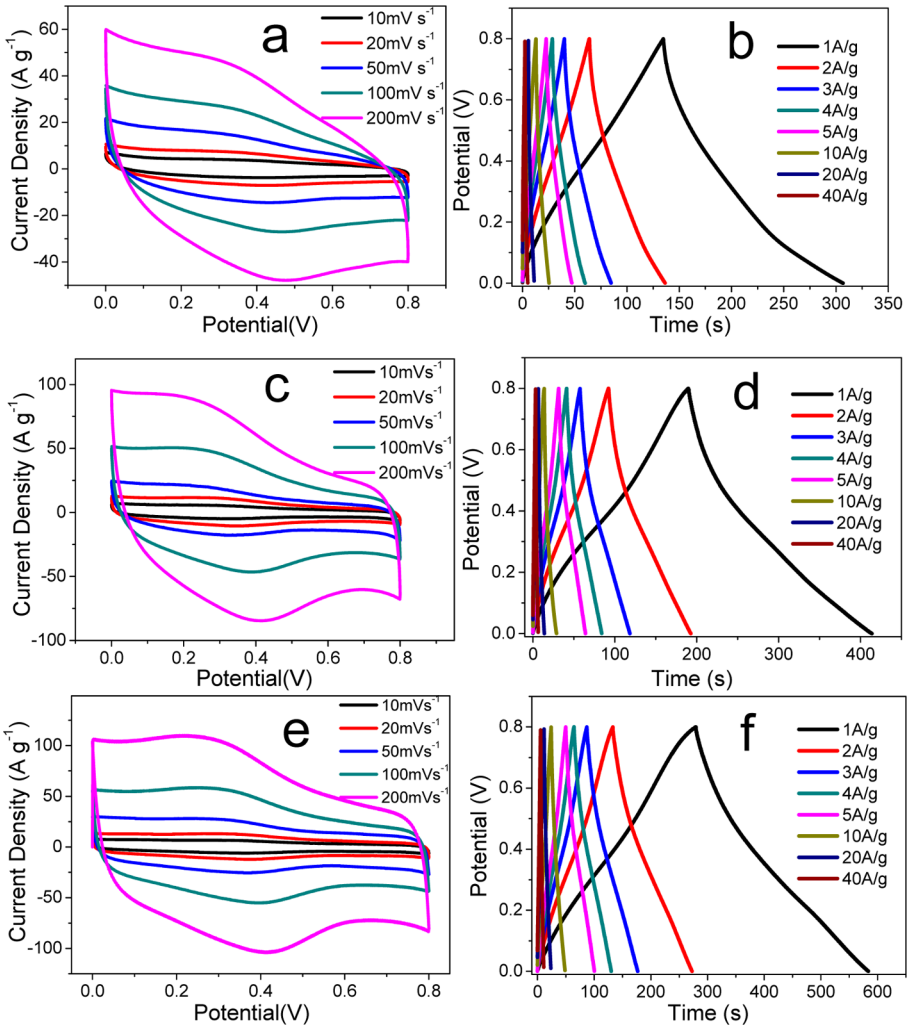

Figure 5. CV curves and galvanostatic charge−discharge curves of (a and b) YS-HCSs, (c and d) SS-HCSs, and (e and f) DS-HCSs.

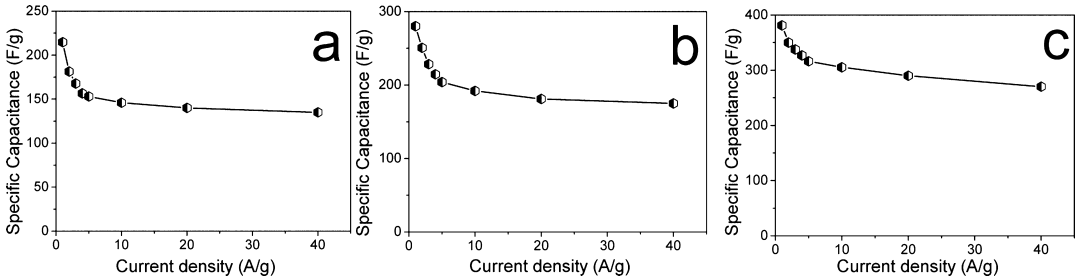

Figure 6. Specific capacitance calculated from galvanostatic charge−discharge curves for (a) YS-HCSs, (b) SS-HCSs, and (c) DS-HCSs.

The supercapacitor performances of the obtained carbon materials were measured by cyclic voltammogram (CV) and galvanostatic charge−discharge. Figure 5a,c,e shows the CV curves of the YS-HCSs, SS-HCSs, and DS-HCSs obtained from a three-electrode cell under a potential window of 0−0.8 V (vs Ag/AgCl) at different scan rates. The rectangular-like shapes and the appearance of humps in the CV curves indicate that the capacitive response comes from the combination of electric double-layer capacitance and redox reactions, which relate to the heteroatom functionalities of the materials. Galvanostatic charge/discharge method is assumed to be the most accurate technique for supercapacitor and applied to calculate the specific capacitances of the three materials. Figure 5b,d,f shows the galvanostatic charge/discharge curves at various current densities (1−40 A g^{-1}). According to the formula $C = It/m\Delta E$(herein, I is the charge/discharge current, t is the discharge time, m is the mass of sample in the electrode, and ΔE is the voltage difference), the specific capacitance of YS-HCSs, SS-HCSs, and DS-HCSs was 215, 280, and 381 F g^{-1}, respectively, at 1A g^{-1}. Even at an extremely high current density of 40 A g^{-1}, the specific capacitances for YS-HCSs, SS-HCSs, and DS-HCSs remain at 63, 62, and 70%, respectively (Figure 6). Through the comparison of the three carbon materials, it can be clearly seen that DS-HCSs show the higher specific capacitance than YS-HCSs and SS-HCSs. It is also important to note that the capacitance value (381 F g^{-1}) obtained for the DS-HCSs at 1A g^{-1} in 1 M H_2SO_4 is

DOI: 10.1021/acsami.5b05035
ACS Appl. Mater. Interfaces 2015, 7, 18609−18617

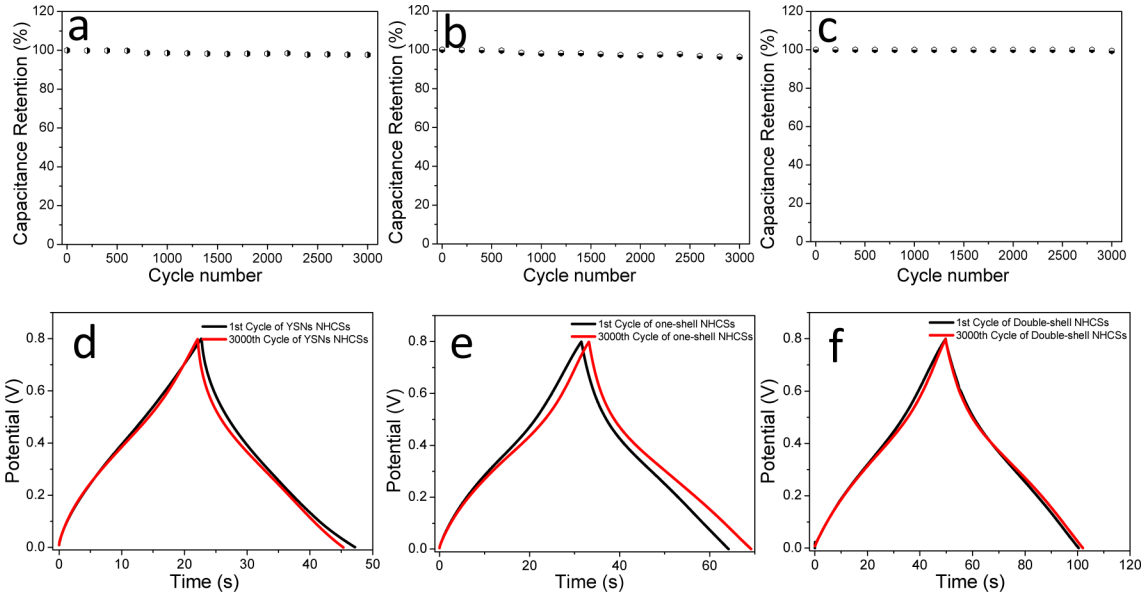

Figure 7. Cycling stability measured for (a) YS-HCSs, (b) SS-HCSs, and (c) DS-HCSs and galvanostatic charge−discharge curves of the first and 3000th cycle for (d) YS-HCSs, (e) SS-HCSs, and (f) DS-HCSs.

higher than that of many types of nitrogen-doped carbon materials, including 3D carbons,[46] nanotubes,[47] nanocages,[48] nanospheres,[49] graphene,[50] and nanofibers.[45] The supercapacitive performances of the materials could be also tested via electrochemical impedance spectra (EIS). Figure S9 is the Nyquist plots of the three N-HCSs materials. The EIS curve of DS-HCSs was much closer to the *y* axis, indicating that DS-HCSs behaved as a more ideal supercapacitor, in accordance with the specific capacitances results. The remarkable specific capacitance of DS-HCSs may be attributed to the high surface area of DS-HCSs, which allows a large amount of electrical charge to accumulate on the electrode/electrolyte interface. The hollow structure is beneficial for electrolyte penetration and can accelerate the kinetic process of the ion transfer within the electrode materials. Nitrogen doping can enhance the electrical conductivity and electrolyte solution wettability of the carbon materials, thereby enhancing the capacitance. Particularly, the double-layered structure generates the voids between the carbon shell, which may provide more active sites and higher volumetric energy density for the electrochemical reactions and tolerate the volume changes during charge/discharge processes.

Cycling performance is another important factor in determining the supercapacitor electrodes for many practical applications. The cycling stability of the three carbon materials electrodes were examined using galvanostatic charge−discharge cycling at a current density of 5 A g^{-1} (Figure 7a−c). During the 3000 cycles, the specific capacitances are almost constant (all the capacitance retentions of the three materials nearly remaining 97%), which demonstrates good cycling performance. This is further confirmed by the inconspicuous change between the charging−discharging curves of the first and 3000th cycle (Figure 7d−f). TEM images of the samples showed that no obvious morphology change was occurred after the cycles, confirming the stability of these three N-HCSs (Figure S10).

4. CONCLUSION

In summary, monodispersed N-doped hollow carbon spheres with yolk−shell, single-shell, and double-shells have been successfully prepared using dopamine (DA) as a carbon precursor and TEOS as a structure-assistant agent in a mixture containing water, ethanol, and ammonia. The structures of the hollow carbon spheres can be efficiently controlled through the adjustment of the amount of ammonia, which can significantly influence the hydrolysis and polymerization rate of TEOS and DA. The three types of carbon spheres obtained using this method, including YS-HCSs, SS-HCSs, and DS-HCSs, exhibit high capacitances of 215, 280, and 381 F g^{-1}, respectively. Moreover, the nitrogen-doped hollow carbon nanospheres showed a good cycling stability 97.0% capacitive retention after 3000 cycles. Notably, the highest capacitance of DS-HCSs up to 381 F g^{-1} is higher than the capacitance reported so far for many carbon-based materials, which may be attributed to the high surface area, hollow structure, nitrogen functionalization, and double-shell architecture. These kinds of N-doped hollow-structured carbon spheres may show promising prospects as advanced energy storage materials and catalyst supports.

■ ASSOCIATED CONTENT

Ⓢ Supporting Information

The Supporting Information is available free of charge on the ACS Publications website at DOI: 10.1021/acsami.5b05035.

TGA curves, N_2 adsorption−desorption isotherm, XPS survey spectrum, Raman spectrum of N-HCSs, TEM images of NCSs, polymer/silica spheres, carbon/silica spheres and silica spheres, N-HCSs after cycles, and electrochemical impedance spectra of N-HCSs (PDF)

■ AUTHOR INFORMATION

Corresponding Authors

*E-mail: lijsh@mail.njust.edu.cn.
*E-mail: wanglj@mail.njust.edu.cn.

Notes

The authors declare no competing financial interest.

■ ACKNOWLEDGMENTS

This work was financially supported by the National Natural Science Foundation of China (Grant No. 51478224) and the

DOI: 10.1021/acsami.5b05035
ACS Appl. Mater. Interfaces 2015, 7, 18609−18617

priority academic program development of Jiangsu higher education institutions.

REFERENCES

(1) Xia, Y. D.; Mokaya, R. Ordered Mesoporous Carbon Hollow Spheres Nanocast Using Mesoporous Silica via Chemical Vapor Deposition. *Adv. Mater.* **2004**, *16*, 886−891.
(2) Yoon, S. B.; Sohn, K.; Kim, J. Y.; Shin, C. H.; Yu, J. S.; Hyeon, T. Fabrication of Carbon Capsules with Hollow Macroporous Core/Mesoporous Shell Structures. *Adv. Mater.* **2002**, *14*, 19−21.
(3) Qiao, Z. A.; Huo, Q. S.; Chi, M. F.; Veith, G. M.; Binder, A. J.; Dai, S. A "Ship-In-A-Bottle" Approach to Synthesis of Polymer Dots@ Silica or Polymer Dots@ Carbon Core-Shell Nanospheres. *Adv. Mater.* **2012**, *24*, 6017−6021.
(4) Lu, A. H.; Li, W. C.; Hao, G. P.; Spliethoff, B.; Bongard, H. J.; Schaack, B. B.; Schuth, F. Easy Synthesis of Hollow Polymer, Carbon, and Graphitized Microspheres. *Angew. Chem., Int. Ed.* **2010**, *49*, 1615−1618.
(5) Qiao, Z. A.; Guo, B. K.; Binder, A. J.; Chen, J. H.; Veith, G. M.; Dai, S. Controlled Synthesis of Mesoporous Carbon Nanostructures via A "Silica-Assisted" Strategy. *Nano Lett.* **2013**, *13*, 207−212.
(6) Yang, T. Y.; Zhou, R. F.; Wang, D. W.; Jiang, S. P.; Yamauchi, Y.; Qiao, S. Z.; Monteiro, M. J.; Liu, J. Hierarchical Mesoporous Yolk-Shell Structured Carbonaceous Nanospheres for High Performance Electrochemical Capacitive Energy Storage. *Chem. Commun.* **2015**, *51*, 2518−2521.
(7) Fang, X. L.; Liu, S. J.; Zang, J.; Xu, C. F.; Zheng, M. S.; Dong, Q. F.; Sun, D. H.; Zheng, N. F. Precisely Controlled Resorcinol−Formaldehyde Resin Coating for Fabricating Core−Shell, Hollow, and Yolk-Shell Carbon Nanostructures. *Nanoscale* **2013**, *5*, 6908−6916.
(8) Liu, R.; Qu, F. L.; Guo, Y. L.; Yao, N.; Priestley, R. D. Au@Carbon Yolk-Shell Nanostructures via One-Step Core-Shell-Shell Template. *Chem. Commun.* **2014**, *5*, 478−480.
(9) Zhang, C. F.; Wu, H. B.; Yuan, C. Z.; Guo, Z. P.; Lou, X. W. Confining Sulfur in Double-Shelled Hollow Carbon Spheres for Lithium-Sulfur Batteries. *Angew. Chem., Int. Ed.* **2012**, *51*, 9592−9595.
(10) Gu, D.; Bongard, H.; Deng, Y. H.; Feng, D.; Wu, Z. X.; Fang, Y.; Mao, J. J.; Tu, B.; Schuth, F.; Zhao, D. Y. An Aqueous Emulsion Route to Synthesize Mesoporous Carbon Vesicles And Their Nanocomposites. *Adv. Mater.* **2010**, *22*, 833−837.
(11) Chen, S. Q.; Huang, X. D.; Sun, B.; Zhang, J. Q.; Liu, H.; Wang, G. X. Multi-Shelled Hollow Carbon Nanospheres for Lithium-Sulfur Batteries with Superior Performances. *J. Mater. Chem. A* **2014**, *2*, 16199−16207.
(12) Wang, G. H.; Sun, Q.; Zhang, R.; Li, W. C.; Zhang, X. Q.; Lu, A. H. Weak Acid-Base Interaction Induced Assembly for The Synthesis of Diverse Hollow Nanospheres. *Chem. Mater.* **2011**, *23*, 4537−4542.
(13) Fang, X. L.; Zang, J.; Wang, X. L.; Zheng, M. S.; Zheng, N. F. A Multiple Coating Route to Hollow Carbon Spheres with Foam-Like Shells and Their Applications in Supercapacitor and Confined Catalysis. *J. Mater. Chem. A* **2014**, *2*, 6191−6197.
(14) Hu, G.; Ma, D.; Cheng, M.; Liu, L.; Bao, X. H. Direct Synthesis of Uniform Hollow Carbon Spheres by A Self-Assembly Template Approach. *Chem. Commun.* **2002**, 1948−1949.
(15) Yang, Z. C.; Zhang, Y.; Kong, J. H.; Wong, S. Y.; Li, X.; Wang, J. Hollow Carbon Nanoparticles of Tunable Size and Wall Thickness by Hydrothermal Treatment of α-cyclodextrin Templated by F127 Block Copolymers. *Chem. Mater.* **2013**, *25*, 704−710.
(16) Lee, H. J.; Choi, S.; Oh, M. Well-Dispersed Hollow Porous Carbon Spheres Synthesized by Direct Pyrolysis of Core-Shell Type Metal-Organic Frameworks and Their Sorption Properties. *Chem. Commun.* **2014**, *50*, 4492−4495.
(17) White, R. J.; Tauer, K.; Antonietti, M.; Titirici, M. M. Functional Hollow Carbon Nanospheres by Latex Templating. *J. Am. Chem. Soc.* **2010**, *132*, 17360−17363.
(18) Ikeda, S.; Tachi, K.; Ng, Y. H.; Ikoma, Y.; Sakata, T.; Mori, H.; Harada, T.; Matsumura, M. Selective Adsorption of Glucose-Derived Carbon Precursor on Amino-Functionalized Porous Silica for Fabrication of Hollow Carbon Spheres with Porous Walls. *Chem. Mater.* **2007**, *19*, 4335−4340.
(19) Ikeda, S.; Ishino, S.; Harada, T.; Okamoto, N.; Sakata, T.; Mori, H.; Kuwabata, S.; Torimoto, T.; Matsumura, M. Ligand-Free Platinum Nanoparticles Encapsulated in a Hollow Porous Carbon Shell as a Highly Active Heterogeneous Hydrogenation Catalyst. *Angew. Chem., Int. Ed.* **2006**, *45*, 7063−7066.
(20) Fuertes, A. B.; Valle-Vigon, P.; Sevilla, M. One-Step Synthesis of Silica@Resorcinol-Formaldehyde Spheres and Their Application for The Fabrication of Polymer and Carbon Capsules. *Chem. Commun.* **2012**, *48*, 6124−6126.
(21) Lu, A. H.; Sun, T.; Li, W. C.; Sun, Q.; Han, F.; Liu, D. H.; Guo, Y. Synthesis of Discrete and Dispersible Hollow Carbon Nanospheres with High Yniformity by Using Confined Nanospace Pyrolysis. *Angew. Chem., Int. Ed.* **2011**, *50*, 11765−11768.
(22) Lou, X. W.; Archer, L. A.; Yang, Z. C. Hollow Micro-/Nanostructures: Synthesis and Applications. *Adv. Mater.* **2008**, *20*, 3987−4019.
(23) Han, Y.; Dong, X. T.; Zhang, C.; Liu, S. X. Hierarchical Porous Carbon Hollow-Spheres as A High Performance Electrical Double-Layer Capacitor Material. *J. Power Sources* **2012**, *211*, 92−96.
(24) Bhattacharjya, D.; Kim, M. S.; Bae, T. S.; Yu, J. S. High Performance Supercapacitor Prepared from Hollow Mesoporous Carbon Capsules with Hierarchical Nanoarchitecture. *J. Power Sources* **2013**, *244*, 799−805.
(25) Xie, K.; Qin, X. T.; Wang, X. Z.; Wang, Y. N.; Tao, H. S.; Wu, Q.; Yang, L. J.; Hu, Z. Carbon Nanocages as Supercapacitor Electrode Materials. *Adv. Mater.* **2012**, *24*, 347−352.
(26) Zhang, L. L.; Zhao, X. S. Carbon-Based Materials as Supercapacitor Electrodes. *Chem. Soc. Rev.* **2009**, *38*, 2520−2531.
(27) Inagaki, M.; Konno, H.; Tanaike, O. Carbon Materials for Electrochemical Capacitors. *J. Power Sources* **2010**, *195*, 7880−7903.
(28) Ferrero, G. A.; Fuertes, A. B.; Sevilla, M. N-Doped Porous Carbon Capsules with Tunable Porosity for High-Performance Supercapacitors. *J. Mater. Chem. A* **2015**, *3*, 2914−2923.
(29) Yuan, C. Q.; Liu, X. H.; Jia, M. Y.; Luo, Z. X.; Yao, J. N. Facile Preparation of N-and O-Doped Hollow Carbon Spheres Derived from Poly (O-Phenylenediamine) for Supercapacitors. *J. Mater. Chem. A* **2015**, *3*, 3409−3415.
(30) Chen, L. F.; Zhang, X. D.; Liang, H. W.; Kong, M. G.; Guan, Q. F.; Chen, P.; Wu, Z. Y.; Yu, S. H. Synthesis of Nitrogen-Doped Porous Carbon Nanofibers as An Efficient Electrode Material for Supercapacitors. *ACS Nano* **2012**, *6*, 7092−7102.
(31) Lee, W. H.; Moon, J. H. Monodispersed N-Doped Carbon Nanospheres for Supercapacitor Application. *ACS Appl. Mater. Interfaces* **2014**, *6*, 13968−13976.
(32) Li, Y.; Li, T. T.; Yao, M.; Liu, S. Q. Metal-Free Nitrogen-Doped Hollow Carbon Spheres Synthesized by Thermal Treatment of Poly(O-Phenylenediamine) for Oxygen Reduction Reaction in Direct Methanol Fuel Cell Applications. *J. Mater. Chem.* **2012**, *22*, 10911−10917.
(33) Han, J. P.; Xu, G. Y.; Ding, B.; Pan, J.; Dou, H.; MacFarlane, D. R. Porous Nitrogen-Doped Hollow Carbon Spheres Derived from Polyaniline for High Performance Supercapacitors. *J. Mater. Chem. A* **2014**, *2*, 5352−5357.
(34) Xia, Y. D.; Yang, Z. X.; Mokaya, R. Mesostructured Hollow Spheres of Graphitic N-Doped Carbon Nanocast from Spherical Mesoporous Silica. *J. Phys. Chem. B* **2004**, *108*, 19293−19298.
(35) Liu, Y. L.; Ai, K. L.; Lu, L. H. Polydopamine and Its Derivative Materials: Synthesis and Promising Applications in Energy, Environmental, and Biomedical Fields. *Chem. Rev.* **2014**, *114*, 5057−5115.
(36) Liang, Y. R.; Liu, H.; Li, Z. H.; Fu, R. W.; Wu, D. C. In Situ Polydopamine Coating-Directed Synthesis of Nitrogen-Doped Ordered Nanoporous Carbons with Superior Performance in Supercapacitors. *J. Mater. Chem. A* **2013**, *1*, 15207−15211.
(37) Tang, J.; Liu, J.; Li, C. L.; Li, Y. Q.; Tade, M. O.; Dai, S.; Yamauchi, Y. Synthesis of Nitrogen-Doped Mesoporous Carbon Spheres with Extra-Large Pores through Assembly of Diblock Copolymer Micelles. *Angew. Chem., Int. Ed.* **2014**, *54*, 588−593.

DOI: 10.1021/acsami.5b05035
ACS Appl. Mater. Interfaces 2015, 7, 18609−18617

(38) Zhou, D.; Yang, L. P.; Yu, L. H.; Kong, J.; Yao, X. Y.; Liu, W. S.; Xu, Z. C.; Lu, X. H. Fe/N/C Hollow Nanospheres by Fe(iii)-Dopamine Complexation-Assisted One-Pot Doping as Nonprecious-Metal Electrocatalysts for Oxygen Reduction. *Nanoscale* **2015**, *7*, 1501−1509.
(39) Zhang, H. W.; Zhou, L.; Noonan, O.; Martin, D. J.; Whittaker, A. K.; Yu, C. Z. Tailoring the Void Size of Iron Oxide@Carbon Yolk−Shell Structure for Optimized Lithium Storage. *Adv. Funct. Mater.* **2014**, *24*, 4337−4342.
(40) Liu, R.; Mahurin, S. M.; Li, C.; Unocic, R. R.; Idrobo, J. C.; Gao, H. J.; Pennycook, S. J.; Dai, S. Dopamine as a Carbon Source: The Controlled Synthesis of Hollow Carbon Spheres and Yolk-Structured Carbon Nanocomposites. *Angew. Chem., Int. Ed.* **2011**, *50*, 6799−6802.
(41) Ai, K. L.; Liu, Y. L.; Ruan, C. P.; Lu, L. H.; Lu, G. Q. Sp2 C-Dominant N-Doped Carbon Sub-micrometer Spheres with a Tunable Size: A Versatile Platform for Highly Efficient Oxygen-Reduction Catalysts. *Adv. Mater.* **2013**, *25*, 998−1003.
(42) Liu, J.; Qiao, S. Z.; Chen, J. S.; Lou, X. W.; Xing, X. R.; Lu, G. Q. Yolk/Shell Nanoparticles: New Platforms for Nanoreactors, Drug Delivery and Lithium-Ion Batteries. *Chem. Commun.* **2011**, *47*, 12578−12591.
(43) Dai, Y. H.; Jiang, H.; Hu, Y. J.; Fu, Y.; Li, C. Z. Controlled Synthesis of Ultrathin Hollow Mesoporous Carbon Nanospheres for Supercapacitor Applications. *Ind. Eng. Chem. Res.* **2014**, *53*, 3125−3130.
(44) Wang, J. X.; Feng, S. S.; Song, Y. F.; Li, W.; Gao, W. J.; Elzatahry, A. A.; Aldhayan, D.; Xia, Y. Y.; Zhao, D. Y. Synthesis of Hierarchically Porous Carbon Spheres with Yolk-Shell Structure for High Performance Supercapacitors. *Catal. Today* **2015**, *243*, 199−208.
(45) Chen, X. Y.; Chen, C.; Zhang, Z. J.; Xie, D. H.; Deng, X.; Liu, J. W. Nitrogen-Doped Porous Carbon for Supercapacitor with Long-Term Electrochemical Stability. *J. Power Sources* **2013**, *230*, 50−58.
(46) Mun, Y.; Jo, C.; Hyeon, T.; Lee, J.; Ha, K.; Jun, K.; Lee, S.; Hong, S.; Lee, H. I.; Yoon, S.; Lee, J. Simple Synthesis of Hierarchically Structured Partially Graphitized Carbon by Emulsion/Block-Copolymer Co-Template Method for High Power Supercapacitors. *Carbon* **2013**, *64*, 391−402.
(47) Tan, Y.; Xu, C.; Chen, G.; Liu, Z.; Ma, M.; Xie, Q.; Zheng, N.; Yao, S. Synthesis of Ultrathin Nitrogen-Doped Graphitic Carbon Nanocages as Advanced Electrode Materials for Supercapacitor. *ACS Appl. Mater. Interfaces* **2013**, *5*, 2241−2248.
(48) Su, F.; Poh, C. K.; Chen, J. S.; Xu, G.; Wang, D.; Li, Q.; Lin, J.; Lou, X. W. Nitrogen-Containing Microporous Carbon Nanospheres with Improved Capacitive Properties. *Energy Environ. Sci.* **2011**, *4*, 717−724.
(49) Dong, X.; Xu, H.; Wang, X.; Huang, Y.; Chan-Park, M.; Zhang, H.; Wang, L.; Huang, W.; Chen, P. 3D Graphene-Cobalt Oxide Electrode for High-Performance Supercapacitor and Enzymeless Glucose Detection. *ACS Nano* **2012**, *6*, 3206−3213.
(50) Jiang, H.; Lee, P. S.; Li, C. 3D Carbon Based Nanostructures for Advanced Supercapacitors. *Energy Environ. Sci.* **2013**, *6*, 41−53.

DOI: 10.1021/acsami.5b05035
ACS Appl. Mater. Interfaces 2015, 7, 18609−18617